



ELSEVIER

Physica E 14 (2002) 341–345

PHYSICA E

www.elsevier.com/locate/physse

UHV compatible nanostructuring technique for mesoscopic hybrid devices: application to superconductor/ferromagnet Josephson contacts

T. Hoss^a, C. Strunk^{a,b,*}, C. Sürgers^c, C. Schönenberger^a

^a*Institut für Physik, Universität Basel, Klingelbergstrasse 82, CH-4065 Basel, Switzerland*

^b*Institut für experimentelle und angewandte Physik, Universität Regensburg, D-93040 Regensburg, Germany*

^c*Physikalisches Institut, Universität Karlsruhe, D-76128 Karlsruhe, Germany*

Received 20 March 2001; received in revised form 9 May 2001; accepted 10 May 2001

Abstract

We report on an ultra-high vacuum (UHV) compatible method for fabricating devices of sub-micrometer size by virtue of a non-organic evaporation mask of high thermal and mechanical stability. As an application we describe the superconducting properties of mesoscopic superconductor/normal-metal and superconductor/ferromagnet/superconductor hybrid structures. In particular, we report on the observation of the DC-Josephson effect in Nb/Cu/Co/Cu/Nb structures prepared in UHV. The Josephson coupling between the two superconductors through the very thin (5 nm) magnetic and metallic weak link is confirmed by the magnetic field dependence of the critical current I_c , which displays a Fraunhofer-like interference pattern. © 2002 Elsevier Science B.V. All rights reserved.

PACS: M73.23.–b; 74.80.Fp; N72.25.–b

Keywords: Nanostructuring; Hybrid devices; Josephson contacts

Electron beam lithography has become the standard technique for sample fabrication in the submicron regime. The fabrication of hybrid structures consisting of several metal layers can be done by using a bilayer resist to prepare a suspended shadow mask. Structures of considerable complexity can be created in a single vacuum run by evaporation under different angles of the vapor beam with respect to the

substrate. So far most, of the work has used resists based on organic polymers, in particular PMMA and PMMA/MA. Such organic resist masks contain solvents which degas in vacuum to a certain extent. This poses a problem for the patterning of highly reactive metals and for the evaporation under UHV conditions. In particular, the vapor deposition of refractory metals such as Nb or Ta gives rise to an excessive increase of degassing because of the very high melting point and the resulting thermal load on the resist [1]. Combined

* Corresponding author.

with the high reactivity of the Nb vapor this leads to a deterioration of the superconducting properties for lateral sample dimensions below 1 μm . Recently, the use of a resist with a substantially higher glass temperature (polyethersulphone) has led to a certain improvement [2].

In this letter, we describe a new approach which completely avoids the limitations of organic resists by using Si_3N_4 as a mask and SiO_2 as a spacer layer, which do not contain any solvents. We apply the technique for the fabrication of superconductor (S)/normal-metal (N) and superconductor/ferromagnet/superconductor (SFS) hybrid structures and demonstrate the possibility of lift-off.

Our fabrication technique is based on a heterostructure consisting of a silicon substrate covered by an 800 nm SiO_2 spacer layer and a 200 nm Si_3N_4 layer for the suspended mask. For the patterning of the mask, 750 nm PMMA is spun on top of the Si_3N_4 and is removed before evaporation. The pattern is written by e-beam lithography into the PMMA which is used as a stencil to transfer the pattern into the nitride layer by reactive ion-plasma etching (100 W RF-power) in a gas mixture of 90% CHF_3 and 10% O_2 at 0.025 mbar. The Si_3N_4 is anisotropically etched at a rate of 35 nm/min. Residual PMMA is subsequently removed by an oxygen plasma. The SiO_2 below the mask can be underetched several micrometers with buffered hydrofluoric acid (BHF) and while the nitride mask remains mechanically very stable. The offset of 800 nm of the mask from the substrate and the large undercut allow substantial relative shifts between the shadow images when evaporating under different angles [3].

For a verification of the mask stability against the thermal load during deposition of high-melting materials we first investigated the transition temperature T_c of narrow Nb wires (thickness $d = 50$ nm) as a function of the wire width [3]. The transition temperature T_c of the polycrystalline samples was 8.4 K and the width of the transition $\simeq 30$ mK in agreement with data obtained on unstructured Nb films of similar thickness on Si without a relevant size dependence down to a wire width of 250 nm. This demonstrates the quality and purity of the Nb in the vicinity of the shadow mask.

A more complicated application is the preparation of SN-hybrid structures [4]. As an example, Fig. 1 shows a single SQUID and a sequence of

16 micro-SQUIDs each comprising two parallel Cu bridges of 1 μm length and 150 nm width between 100 nm thick Al banks before and after lift-off. The lift-off, i.e., the mechanical removal of the shadow mask, is done by spinning several layers of dilute PMMA on the sample and lift-off together with the mask. This works reliably for all 16 junctions (see Fig. 1(c), (d)). The magnetoresistance of the device shows oscillations with a period of 53 mT. This agrees well with the period of 55 mT expected from the area of the single SQUID loops.

In the following we will focus on another application, i.e., the preparation of planar SFS microjunctions which are presently attracting considerable interest [5,6]. The distinct feature of a SFS junction is a possible sign change of the order parameter difference for certain values of the ratio d/ξ_F , where d is the thickness of the F interlayer and ξ_F is the (complex) penetration depth of the Cooper pair amplitude \mathcal{F} in the F layer: $\mathcal{F}(x) \propto \exp(-x/\xi_F)$ with $\xi_F^2 = -i\hbar D/2I_{\text{ex}}$ and I_{ex} being the exchange energy in ferromagnet. This simple formula holds in the dirty limit and when $I_{\text{ex}} \gg k_B T$. The oscillatory component of F is caused by the interference of the spin-split $k_{F\uparrow}$ and $k_{F\downarrow}$ electrons forming the pairs.

The oscillatory behavior of F should appear in the thickness dependence of $T_c(d_F)$ and $I_c(d_F)$ [7,8]. While $T_c(d_F)$ gives less direct evidence for the oscillation of $F(x)$, [9–13] $I_c(d_F)$ is expected to probe the sign changes of $F(x)$ [8]. The modulus of the decay length $|\xi_F|$ is of the order of 1–2 nm in concentrated ferromagnets. In order to keep d_F in the order of ξ_F the films have to be extremely thin with a correspondingly small resistance. This makes transverse transport measurements difficult unless the junction area is of mesoscopic size.

Fig. 2 shows a scanning electron micrograph of a planar SFS junction together with a schematic to illustrate the stacking sequence and the junction geometry. The individual layers were deposited by e-beam evaporation in UHV (base pressure $\leq 10^{-10}$ mbar). First, 40 nm Nb (S_1) was deposited with a 15° angle between the sample normal and the vapor beam. In a second step, a triple layer of Cu/Co/Cu (5 nm each) was deposited from the left under an angle of 53° . This large angle ensures that the edge of the Nb film is homogeneously covered. The Cu serves as a buffer layer to reduce the roughness of the polycrystalline Nb film

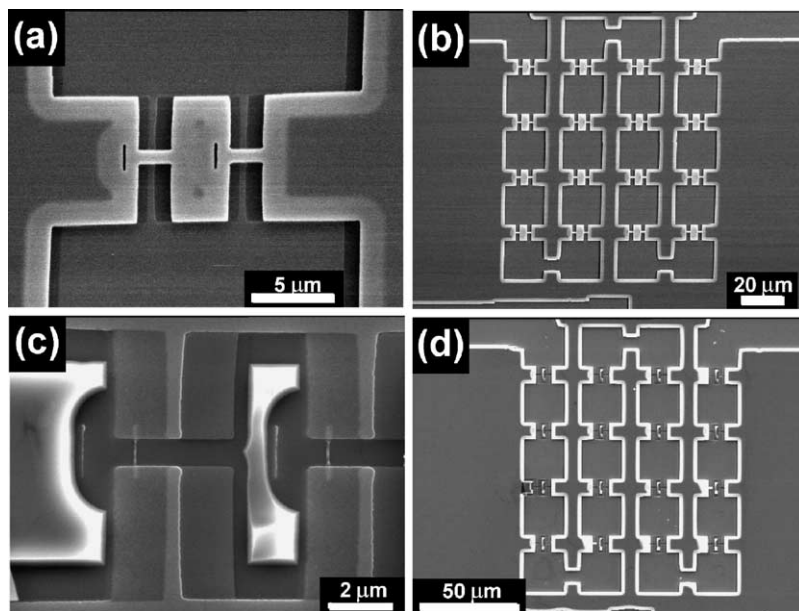


Fig. 1. Free standing Si_3N_4 mask with an offset of 800 nm from the substrate for shadow evaporation of a single SQUID (a) and a SN multi-SQUID device (b). Cu (N) was evaporated from the left direction followed by Al (S) from the right. This results in two parallel Cu wires between Al reservoirs. (c), (d) Sample after a mechanical lift-off.

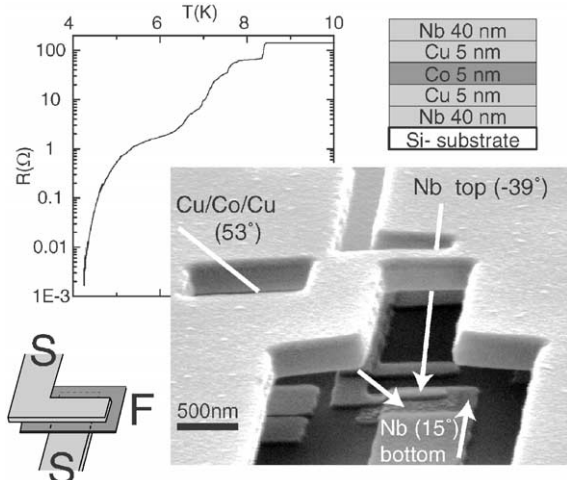


Fig. 2. SFS junction realized in a microstructured Nb/Cu/Co/Cu/Nb multilayer. A very small contact area $360 \times 460 \text{ nm}^2$ is achieved by evaporating the layers under three different angles through a Si_3N_4 -mask. The mask has a distance of 800 nm from the substrate. The arrows indicate the directions of evaporation as described in the text. The top left plot shows $\log R$ vs. T .

before depositing Co and is thin enough not to affect the superconducting properties of the junction. The lateral junction size is $360 \times 460 \text{ nm}^2$ with an overall rms roughness of 1.9 and 1.4 nm for the Nb and Cu film, respectively, as determined by in situ STM investigations on unstructured films prepared under identical conditions. The 5 nm Co film has a rms surface roughness of 0.9 nm and is free of detectable pin holes as inferred from the absence of the Nb (167 eV) and Cu (918 eV) lines in the Auger spectrum taken after Co deposition. Finally, 40 nm Nb (S_2) was deposited under an angle of -39° .

Magnetic hysteresis loops of several Co (F) films deposited on a Cu/Nb bilayer were taken by means of the transverse magneto-optic Kerr effect and by vibrating sample magnetometry with the magnetic field oriented in the film plane. At temperatures below 10 K coercive fields of 5.3 mT ($d_F = 5 \text{ nm}$), 12 mT ($d_F = 3 \text{ nm}$), and 28 mT ($d_F = 1 \text{ nm}$), and a saturation magnetization close to the bulk value were measured. The coercivity of the $1 \times 1 \mu\text{m}^2$ Co interlayer in the SFS sample may be slightly higher because of finite size effects.

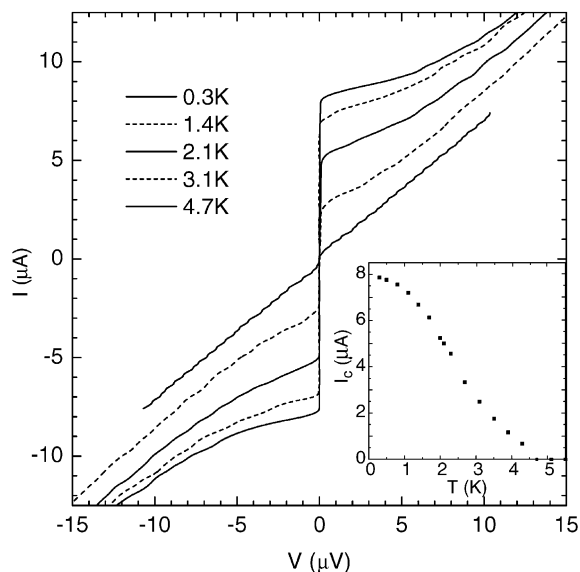


Fig. 3. IV characteristics of the SFS-junction in Fig. 2 for different temperatures. Inset: Critical current I_c vs. temperature T .

Electrical transport measurements were performed in a [3] He-cryostat with elaborate RF-filtering of the electrical leads at the cryostat head and at the sample stage. In the normal state the two-point resistance of the sample including the leads on the chip was 141Ω . The plot in Fig. 2 shows that below 8.4 K the resistance $R(T)$ drops in several steps down to $\approx 2 \Omega$ at 6.2 K. These steps are caused by the different sections of the leads on the chip which—depending on their width—may or maynot contain a Co interlayer. In the former case the transition temperature is suppressed also in the leads. Around 6 K, the resistance develops a broad shoulder and drops another three orders of magnitude at lower temperatures. The normal state resistance of the junction at 6 K is 1.8Ω .

Fig. 3 shows the current–voltage (IV) characteristics of the junction at different temperatures. We find a well defined critical current of about $8 \mu\text{A}$ at 0.3 K which vanishes above 4.7 K. $I_c(0.3 \text{ K})$ is much smaller than the Kulik–Omelyanchuk result [14] of $I_c(0) = a \times \pi \Delta(0) / 2eR_N \approx 3 \text{ mA}$ for SNS junctions, where a is of order unity. This indicates the strong pair breaking effect of the 5 nm Co interlayer. The inset shows the temperature dependence of the critical current. Unlike in the experiment of Ryazanov et al. [5] we do not observe a transition from a “0”-state to a

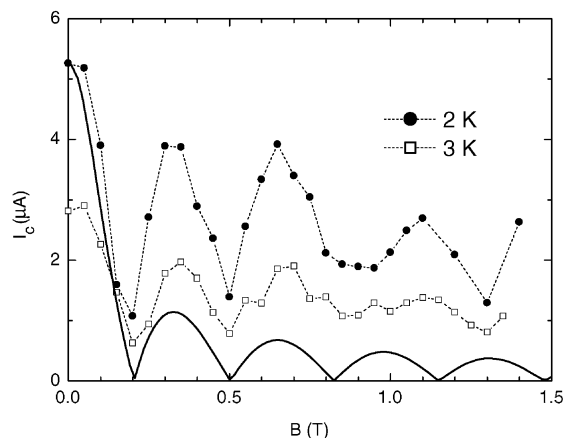


Fig. 4. Critical current I_c vs. magnetic field B of the microstructured SFS junction. Solid line: Fraunhofer fit including the magnetization contribution of the Co layer to the enclosed flux.

“ π ”-state as the temperature is varied but a monotonic drop of I_c . This is expected, since we have a concentrated ferromagnet, where $I_{\text{ex}} \gg k_B T$. At temperatures above 2 K we observe an unusual negative curvature, which is currently not understood. The latter was also observed on SFS junctions with a dilute F layer not showing a “0” to “ π ” transition [5].

An important test for the homogeneity of the junction is the observation of an interference pattern of I_c in a magnetic field B applied parallel to the junction as presented in Fig. 4. We find pronounced and relatively regular oscillations of I_c . However, a quantitative analysis shows deviations when compared to an ideal Fraunhofer pattern. These cannot be related to screening effects, since the Josephson penetration depth of the junction is estimated to be $10 \mu\text{m}$ at $T = 0.3 \text{ K}$, i.e. much larger than the junction size. The first minimum of the interference pattern is found at $B \approx 0.2 \text{ T}$, while the second and third minima have a spacing of 0.33 T . This can be explained by taking into account the contribution of the Co layer magnetization to the magnetic flux Φ in the junction. The solid line is a Fraunhofer pattern calculated for a single Josephson junction including the contribution of the Co film.¹ For our film thickness, the effective thickness of the junction depends very weakly on the mag-

¹ We assumed bulk Co values for the saturation magnetization of the film.

netic penetration depth $\lambda(0) \simeq 90$ nm and is given by $d_{\text{eff}} = [2\lambda \tanh[(d_{\text{Nb}} + d_{\text{Cu}})/(2\lambda)] + d_F \simeq 49$ nm [15]. This results in a cross-section of $460 \text{ nm} \times 49 \text{ nm}$ exposed perpendicular to the field and an expected magnetic field period of $\Delta B = 92$ mT substantially smaller than the experimentally observed value of $\Delta B = 330$ mT. This could be related to the stray fields of the Nb layer on the nitride mask at $1 \mu\text{m}$ distance from the junction. Such stray fields can be avoided in future samples designed to allow for lift-off.

The secondary maxima of the diffraction pattern are higher in amplitude than those of the Fraunhofer pattern, while I_c is not exactly zero at half integer values of Φ/Φ_0 , where $\Phi_0 = h/2e$. This indicates that the junction has a certain inhomogeneity, which is not surprising when taking into account the exponential dependence of I_c on d_F and the relatively large relative fluctuations of d_F ($\simeq 30\%$) inferred from the structural characterization. This problem should be strongly reduced when using diluted ferromagnets as in Ref. [5].

In conclusion, we have demonstrated the possibility of fabricating suspended shadow masks suitable for angular evaporation of refractory metals under UHV conditions. This technique allows the preparation of metallic heterostructures with small cross-section and

very thin interlayers. As a promising application, we have demonstrated the DC-Josephson effect in a microfabricated planar junction with a ferromagnetic weak link.

We thank E. Scheer and H.v. Löhneysen for useful discussions and C. Hauschel for help with the experiment. This work was partially supported by the Swiss National Science foundation and the Deutsche Forschungsgemeinschaft through SFB 195.

References

- [1] Y. Harada, et al., *Appl. Phys. Lett.* 65 (1994) 636.
- [2] P. Dubos, et al., *J. Vac. Sci. Technol. B* 18 (2000) 122.
- [3] T. Hoss, C. Strunk, C. Schönenberger, *Microelectron. Eng.* 46 (1999) 149.
- [4] T. Hoss, et al., *Phys. Rev. B* 62 (2000) 4079.
- [5] V.V. Ryazanov, et al., *Phys. Rev. Lett.* 86 (2001) 2427.
- [6] O. Bourgeois, et al., *Phys. Rev. B* 63 (2001) 064517.
- [7] Z. Radovic, et al., *Phys. Rev. B* 44 (1991) 759.
- [8] A.I. Buzdin, M. Kuprianov, *JETP Lett.* 53 (1991) 321.
- [9] C. Strunk, et al., *Phys. Rev. B* 49 (1994) 4053.
- [10] J.S. Jiang, et al., *Phys. Rev. Lett.* 74 (1995) 314.
- [11] J.S. Jiang, et al., *Phys. Rev. B* 54 (1996) 6119.
- [12] Th. Mühge, et al., *Phys. Rev. Lett.* 77 (1996) 1857.
- [13] Th. Mühge, et al., *Phys. Rev. B* 55 (1997) 8945.
- [14] I.O. Kulik, A. Omelyanchuk, *JETP Lett.* 21 (1975) 96.
- [15] M. Weihnacht, *Phys. Status Solidi* 32 (1969) K169.